

## **Copyright Warning & Restrictions**

The copyright law of the United States (Title 17, United States Code) governs the making of photocopies or other reproductions of copyrighted material.

Under certain conditions specified in the law, libraries and archives are authorized to furnish a photocopy or other reproduction. One of these specified conditions is that the photocopy or reproduction is not to be “used for any purpose other than private study, scholarship, or research.” If a user makes a request for, or later uses, a photocopy or reproduction for purposes in excess of “fair use” that user may be liable for copyright infringement,

This institution reserves the right to refuse to accept a copying order if, in its judgment, fulfillment of the order would involve violation of copyright law.

**Please Note: The author retains the copyright while the New Jersey Institute of Technology reserves the right to distribute this thesis or dissertation**

Printing note: If you do not wish to print this page, then select “Pages from: first page # to: last page #” on the print dialog screen

The Van Houten library has removed some of the personal information and all signatures from the approval page and biographical sketches of theses and dissertations in order to protect the identity of NJIT graduates and faculty.

## INFORMATION TO USERS

This material was produced from a microfilm copy of the original document. While the most advanced technological means to photograph and reproduce this document have been used, the quality is heavily dependent upon the quality of the original submitted.

The following explanation of techniques is provided to help you understand markings or patterns which may appear on this reproduction.

1. The sign or "target" for pages apparently lacking from the document photographed is "Missing Page(s)". If it was possible to obtain the missing page(s) or section, they are spliced into the film along with adjacent pages. This may have necessitated cutting thru an image and duplicating adjacent pages to insure you complete continuity.
2. When an image on the film is obliterated with a large round black mark, it is an indication that the photographer suspected that the copy may have moved during exposure and thus cause a blurred image. You will find a good image of the page in the adjacent frame.
3. When a map, drawing or chart, etc., was part of the material being photographed the photographer followed a definite method in "sectioning" the material. It is customary to begin photoing at the upper left hand corner of a large sheet and to continue photoing from left to right in equal sections with a small overlap. If necessary, sectioning is continued again — beginning below the first row and continuing on until complete.
4. The majority of users indicate that the textual content is of greatest value, however, a somewhat higher quality reproduction could be made from "photographs" if essential to the understanding of the dissertation. Silver prints of "photographs" may be ordered at additional charge by writing the Order Department, giving the catalog number, title, author and specific pages you wish reproduced.
5. PLEASE NOTE: Some pages may have indistinct print. Filmed as received.

**Xerox University Microfilms**

300 North Zeeb Road  
Ann Arbor, Michigan 48106

---

7815892

CHU, KERRY KIER-TEN  
DYNAMICS OF SUBMERGED CYLINDRICAL SHELLS WITH  
ECCENTRIC STIFFENING,

NEW JERSEY INSTITUTE OF TECHNOLOGY,  
D.ENG.SC., 1978

University  
Microfilms  
International 300 N. ZEEB ROAD, ANN ARBOR, MI 48106

---

© 1978

PEACE DAY WEIGH

ALL RIGHTS RESERVED

DYNAMICS OF SUBMERGED CYLINDRICAL SHELLS

WITH ECCENTRIC STIFFENING

BY

KERRY KIER-TEN CHU

A DISSERTATION

PRESENTED IN PARTIAL FULFILLMENT OF

THE REQUIREMENTS FOR THE DEGREE

OF

DOCTOR OF ENGINEERING SCIENCE

AT

NEW JERSEY INSTITUTE OF TECHNOLOGY

This dissertation is to be used only with due regard to the rights of the author. Bibliographical references may be noted, but passages must not be copied without permission of the Institute and without credit being given in subsequent written or published work.

Newark, New Jersey

1978

APPROVAL OF DISSERTATION  
DYNAMICS OF SUBMERGED CYLINDRICAL SHELLS  
WITH ECCENTRIC STIFFENING

BY

KERRY KIER-TEN CHU

FOR

DEPARTMENT OF MECHANICAL ENGINEERING  
NEW JERSEY INSTITUTE OF TECHNOLOGY

BY

FACULTY COMMITTEE

APPROVED: \_\_\_\_\_, Chairman

\_\_\_\_\_  
\_\_\_\_\_  
\_\_\_\_\_  
\_\_\_\_\_

NEWARK, NEW JERSEY

May, 1978

## ABSTRACT

A theoretical analysis is presented for treating the free vibrations of submerged, ring stiffened cylindrical shells with simply supported ends. The effects of the eccentric stiffeners are averaged over the thin-walled isotropic cylindrical shell. The energy method is utilized and the frequency equation is derived by Hamilton's Principle. All three degrees of freedom are considered. Numerical results are presented for frequencies and mode separation for several cases of interest. Comparisons with previous theoretical and experimental results indicate good agreement. The cylindrical wave approximation and the plane wave approximation for the field equation were investigated. Their applicability was evaluated and the results indicate that only the cylindrical wave approximate method gives good agreement with the exact solution. For a steel shell in water with  $c = 5.82$  slug/sec, the plane wave approximate method gives very poor results (about 5-20% accuracy)

## ACKNOWLEDGEMENTS

The author wishes to express his sincere appreciation to his advisor, Professor Michael Pappas, for suggesting the topic of this dissertation and for his invaluable assistance and guidance during the author's doctoral research at the New Jersey Institute of Technology. Special acknowledgement goes to Professor Harry Herman for the help provided to solve the approximate solutions. The author is also grateful to the other members of his committee, Professors A. Allentuch, I. Cochin and E. Golub for their advice and comments.

The assistance offered by Dr. E. A. Bulanowski, Chief Engineer, Solid Mechanics Group, Research and Advanced Product Development of Delaval Turbine, Inc. is very much appreciated. The author also wishes to thank Mr. Thomas Chubb, Manager of Fan Technology and Development of The Green Fan Company, for reading the manuscript. Thanks are also due to my colleagues at Delaval Turbine, Inc.: Mr. M. Grove for his valuable suggestions, Miss Alice M. Smith for her assistance in the numerical calculations, and Mrs. Rita Peters for the excellent typing in spite of the difficult notations.



DEDICATION

In memory of my wife

Maimy Pearl

February 16, 1940-March 22, 1977

How happy she would be to see this degree awarded.

TABLE OF CONTENTS

| <u>Chapter</u> | <u>Title</u>  | <u>Page</u> |
|----------------|---|-------------|
|                | LIST OF FIGURES .....   | iii         |
|                | LIST OF TABLES .....  | iv          |
|                | NOMENCLATURE .....  | v           |
| 1              | INTRODUCTION .....  | 1           |
| 2              | GOVERNING FIELD EQUATIONS .....   | 4           |
| 3              | ENERGY OF THE STIFFENED STRUCTURE .....   | 11          |
|                | Potential Energy .....  | 11          |
|                | Kinetic Energy .....  | 17          |
| 4              | EQUATION DERIVATION & NUMERICAL RESULTS....                                       | 20          |
|                | Equation of Motion and<br>Boundary Conditions .....                               | 20          |
|                | Vibration Equations .....   | 26          |
|                | Frequency Equation Derivation .....   | 32          |
|                | Mode Separation .....   | 39          |
|                | Numerical Procedures .....  | 40          |
|                | Comparison with McElman's Method .....  | 41          |
|                | Comparison with Experiments Conducted<br>in Water by Norfolk Naval Shipyard ..... | 44          |

| <u>Chapter</u> | <u>Title</u>   | <u>Page</u> |
|----------------|--|-------------|
|                | Comparison with Experiments<br>Conducted in Air by Hayek & Pallett ..... | 47          |
|                | Mode Separation .....  | 49          |
| 5              | APPROXIMATE SOLUTIONS .....  | 51          |
|                | Plane Wave Approximation .....   | 54          |
|                | Parametric Study .....   | 56          |
| 6              | CONCLUSIONS .....  | 59          |
| 7              | RECOMMENDATION .....   | 61          |
|                | REFERENCES .....   | 62          |
|                | VITA .....   | 65          |

LIST OF FIGURES

| <u>Figure</u> |   | <u>Page</u> |
|---------------|---|-------------|
| 2.1           | Geometry of Ring Stiffened Cylinder ..... | 5           |
| 2.2           | Shock Wave Movement .....                 | 10          |
| 3,1           | Stiffener Geometry .....                  | 12          |
| 5.1           | The After-Flow Coefficient .....          | 58          |

LIST OF TABLES

| <u>Table</u> |  | <u>Page</u> |
|--------------|--|-------------|
| I            | Natural Frequencies (Hz) Comparison<br>with McElman's Method .....     | 43          |
| II           | Natural Frequencies (Hz) Comparison<br>with Underwater Test Data ..... | 46          |
| III          | Natural Frequencies (Hz) Comparison<br>with Air Test Data .....        | 48          |
| IV           | Mode Separation .....  | 50          |

NOMENCLATURE

| <u>Symbol</u>   | <u>Description</u>   |
|-----------------|--|
| $A_0$           | - Fourier coefficient.   |
| $A_r$           | - Cross-sectional area of stiffener  |
| [A]             | - Frequency determinant.   |
| $A_{ij}$        | - Elements of frequency determinant.   |
| c               | - Acoustic velocity in the fluid.  |
| D               | - Flexural stiffness of isotropic cylinder wall,<br>$\frac{Et^3}{12(1 - \nu^2)}$ |
| E               | - Young's modulus.   |
| $\bar{e}$       | - Distance from cylinder middle surface to line on which $\bar{N}_x$ acts.       |
| $F_i$           | - Defined by equation (3.21).  |
| G               | - Shear modulus.   |
| $H_0^{(1)}(KR)$ | - Hankel function of the first kind, of order zero and argument KR.              |
| $H_n^{(1)}(KR)$ | - Hankel function of the first kind, of order n argument KR.                     |
| h               | - Thickness of cylinder.   |
| $h_i$           | - Stiffener dimension as shown in Figure 3.1.                                    |
| I               | - Moment of inertia of stiffener about its centroid.                             |
| $I_0$           | - Moment of inertia of stiffener about middle surface of cylinder.               |
| J               | - Torsional constant for stiffener.  |

|                 |  |
|-----------------|--|
| $K_0(\bar{K}R)$ | - Modified Bessel function of the second kind, of order zero and argument $\bar{K}R$ . |
| $K_n(\bar{K}R)$ | - Modified Bessel function of the second kind, of order $n$ and argument $\bar{K}R$ .  |
| $K, \bar{K}$    | - Coefficient of the equation for potential fluid flow.                                |
| $L$             | - Length of cylindrical shell.   |
| $l$             | - Ring spacing (see Figure 2.1).   |
| $\bar{M}$       | - Mass per unit area.  |
| $M_x$           | - Moment resultant in axial direction.   |
| $M_y$           | - Moment resultant in circumferential direction.                                       |
| $M_{xy}$        | - Shear moment resultant.  |
| $M_{yx}$        | - Shear moment resultant.  |
| $m$             | - Number of longitudinal half-waves.   |
| $N_x$           | - Stress resultant in axial direction.   |
| $N_y$           | - Stress resultant in circumferential direction.                                       |
| $N_{xy}$        | - Shear stress resultant.  |
| $\bar{N}_x$     | - Externally applied load resultant in $x$ direction.                                  |
| $\bar{N}_y$     | - Circumferential stress resultant due to applied pressure.                            |
| $n$             | - Number of circumferential waves.   |
| $P$             | - Total pressure.  |
| $P_h$           | - Hydrostatic pressure.  |
| $P_i$           | - Incident pressure.   |
| $P_r$           | - Radiated pressure.   |
| $\bar{P}_r$     | - The amplitude of the radial pressure.  |

|  |   |
|--|---|
| $R$  | - Radius to middle surface of isotropic cylinder.   |
| $T$  | - Kinetic energy.   |
| $t$  | - Time variable.  |
| $V$  | - Potential energy.   |
| $u, v, w$                                    | - Displacements in $x, y$ , and $z$ directions, respectively (axial, tangential and radial).              |
| $x, y, z$                                    | - Orthogonal coordinates defined in Figure 2.1 ( $x$ and $y$ lie in middle surface of cylinder or plate). |
| $\bar{U}, \bar{V}, \bar{W}$                  | - The amplitudes of displacement.   |
| $\bar{z}$                                    | - Distance from middle surface of cylinder to centroid of stiffener.                                      |
| $\epsilon_x, \epsilon_y, \gamma_{xy}$        | - Membrane normal strains and shearing strain.  |
| $\epsilon_{xT}, \epsilon_{yT}, \gamma_{xyT}$ | - Normal strains and shearing strain.   |
| $\Lambda_i$                                  | - Defined by equation (4.22).   |
| $\mu$  | - Poisson's ratio.  |
| $\omega$                                     | - Circular frequency.   |
| $\rho$                                       | - Density.  |
| $\phi$                                       | - Velocity potential function.  |
| $\Phi$                                       | - The amplitude of the velocity potential.  |

### Subscripts

|     |            |
|-----|------------|
| $c$ | - cylinder |
| $i$ | - Integer  |
| $j$ | - Integer  |



- r - Stiffening in y direction.
- w - Water.
- A - Prestress state.
- B - Small changes away from prestress state.

A comma indicates partial differentiation with respect to the subscript following the comma.

## CHAPTER 1

### INTRODUCTION

Since the early efforts of Rayleigh [1]<sup>1</sup> and Love [2], the vibration of shells in a vacuum has been extensively analyzed. More recently, the prestressed, eccentrically stiffened, cylindrical shell of finite length was investigated by McElman et al [3] and Harari and Baron [4].

The dynamic interaction between shells and fluids has also received considerable attention. Junger [5, 6, 7] was the first to analyze the free and forced vibrations of a cylindrical shell submerged in an acoustic medium. He treated an infinitely long, cylindrical shell utilizing plain strain analysis. The transient response of a submerged infinitely long, ring-stiffened cylindrical shell has been studied by Herman and Klosner [8] and Lyons et al [9]. A submerged cylindrical shell of infinite length, having radial surface motion over a stiffened, finite section has been studied by Paslay et al [10].

Due to the rapid development of deep sea oil drilling, long-range submarine and undersea research, interest has increased in the natural frequency of a submerged, stiffened,

---

<sup>1</sup>Numbers in brackets designate references.

cylindrical shell of finite length. There is no existing analysis method to meet this demand. Therefore, the main objective of the present study is to extend McElman's work for the submerged condition.

A submerged, eccentrically stiffened, cylindrical shell of finite length is analyzed to obtain its natural frequency. The effects of eccentric stiffeners are averaged over the thin-walled isotropic cylindrical shell. Three degrees of vibration of the structure are considered. Boundary conditions are established and satisfied at the fluid-structure interface. In obtaining the frequency equation for the vibration of the eccentric ring-stiffened, submerged, cylindrical shell, the derivation is accomplished by defining the Donnell type of nonlinear strain displacements for the shell and its stiffeners, formulating the potential and kinetic energies of the system, and then applying Hamilton's Principle. A set of appropriate nonlinear equilibrium equations and boundary conditions are derived. The nonlinear equations are used to derive linear equations that govern the small vibration of the system.

Finally, a three degree freedom frequency equation is obtained for the submerged, eccentric ring-stiffened, cylindrical shell. The frequencies are numerically resolved. a value of the has been obtained, the corresponding ratios of radial, axial and tangential amplitudes can be evaluated.

The numerical results obtained from the present analysis for several cases of interest are given in Chapter 3. Good agreement is found with other theoretical investigations and experimental results.

The cylindrical wave approximation and the plane wave approximation for the field equation were investigated and a parametric study was done in order to compare the approximate methods with the exact solution.

## CHAPTER 2

GOVERNING FIELD EQUATIONS

The well known field equation for a homogeneous fluid medium [11] is

$$\nabla^2 \phi = \frac{1}{c^2} \frac{\partial^2 \phi}{\partial t^2}$$

The axisymmetric form of this equation is

$$\frac{\partial^2 \phi}{\partial r^2} + \frac{1}{r} \frac{\partial \phi}{\partial r} + \frac{\partial^2 \phi}{\partial x^2} = \frac{1}{c^2} \frac{\partial^2 \phi}{\partial t^2} \quad (2.1)$$

in which  $\phi$  is the velocity potential function,  $c$  is the velocity of sound in the fluid,  $t$  is the time variable,  $x$  is the shell coordinate parallel to the axis of the structure (Figure 2.1), and  $r$  is the variable describing the distance from the shell surface into the fluid.

The velocity potential,  $\phi$ , and the radiated pressure,  $P_r$ , can be written as

$$\phi = e^{i\omega t} \phi \cos \frac{nY}{R} \sin \frac{mX}{L} \quad (2.2)$$

$$P_r = e^{i\omega t} \bar{P}_r \cos \frac{nY}{R} \sin \frac{mX}{L} \quad (2.3)$$

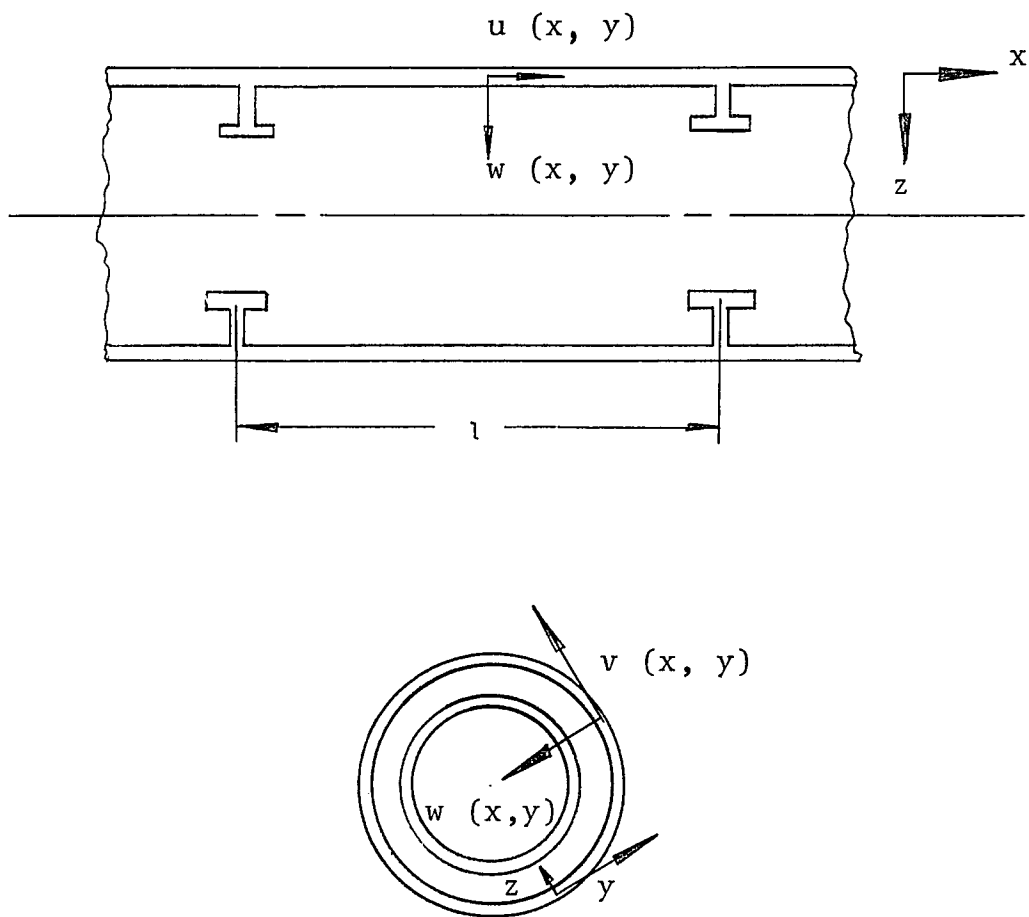


Figure 2.1 - Geometry of Ring Stiffened Cylinder

in which  $\phi$  is the amplitude of the velocity potential,  $\bar{P}_r$  is the amplitude of the radial pressure,  $\omega$  is the circular frequency,  $m$  is the number of axial half-waves,  $n$  is the mean radius of the cylindrical shell, and  $L$  is the length of the cylindrical shell.

Substituting equation (2.2) into the governing field equation (2.1) for the fluid medium yields:

$$\frac{\partial^2 \phi}{\partial r^2} + \frac{1}{r} \frac{\partial \phi}{\partial r} + \left( \frac{\omega^2}{c^2} - \frac{n^2}{R^2} - \frac{m^2 \pi^2}{L^2} \right) \phi = 0$$

Let

$$K^2 = \left( \frac{\omega}{c} \right)^2 - \left( \frac{n}{R} \right)^2 - \left( \frac{m\pi}{L} \right)^2 \quad (2.4)$$

If the fluid is assumed to be infinitely extended, the solution of equation (2.4) for an outgoing wave is given by

$$\phi = A_0 H_0^{(1)}(KR) \quad (2.5)$$

in which  $H_0^{(1)}$  is the Hankel function of the first kind of order zero.

The constant  $A_0$  is evaluated by ensuring that the velocity of the shell and the velocity of the fluid medium are equal at the shell-fluid interface,  $r = R$ , i.e.

$$\frac{\partial w}{\partial t} = \frac{\partial \phi}{\partial r} \quad (2.6)$$

For a shell simply supported at each end, the radial deflection is assumed to be

$$w = \bar{W} e^{i\omega t} \sin \frac{m x}{L} \cos \frac{n y}{R} \quad (2.7)$$

in which  $\bar{W}$  = the amplitude of the radial deflection.

Substituting equations (2.3) and (2.7) into equation (1.6) results in

$$i\omega \bar{W} = \frac{\partial \phi}{\partial r} \quad (2.8)$$

Upon substituting equation (2.5) into equation (2.8), the constant  $A_0$  can be written as

$$A_0 = \frac{-i\omega \bar{W}}{K H_1^{(1)}(KR)} \quad (2.9)$$



The radiated pressure  $P_r$  is defined by the velocity potential of the fluid medium

$$P_r = \rho_w \frac{\partial \phi}{\partial t} \quad (2.10)$$

in which  $\rho_w$  is the density of the fluid. Then

$$P_r = \rho_w \omega^2 e^{i\omega t} f(\omega) \bar{W} \sin \frac{mx}{L} \cos \frac{ny}{R} \quad (2.11)$$

in which

$$\bar{P}_r = \rho_w \omega^2 \bar{W} f(\omega) \quad (2.12)$$

$$f(\omega) = \frac{H_0(KR)}{KH_1^{(1)}(KR)} \quad (2.13)$$

Let

$$K = i\bar{K} = i \sqrt{\left(\frac{m\pi}{L}\right)^2 + \left(\frac{n}{R}\right)^2 - \left(\frac{\omega}{c}\right)^2} \quad (2.14)$$

The function  $f(\omega)$  can be written as

$$f(\omega) = \frac{K_0(\bar{K}R)}{\bar{K} K_1(\bar{K}R)} \quad (2.15)$$

in which  $K_0$  and  $K_1$  are modified Bessel functions of the second kind, of order 0 and 1, respectively.

The shell is assumed to be acted upon by a shock wave which induces a radiated pressure and a hypothetical incident pressure. The radiated pressure is defined by the velocity potential of the acoustic medium and the incident pressure  $P_i$  on the shell is dependent upon the motion of wave front which is shown in Figure 2.2.

For the transient condition, the time  $t$  is equal or less than the value  $\frac{2R}{c}$ . The condition under consideration in this steady-state analysis is that the time  $t$  is greater than the value  $\frac{2R}{c}$ . The wave front has completely passed the cylinder and the incident pressure  $P_i$  may be treated as a constant. The fluid effects at the end of the cylinder were neglected so that the problem is more tractable analytically.

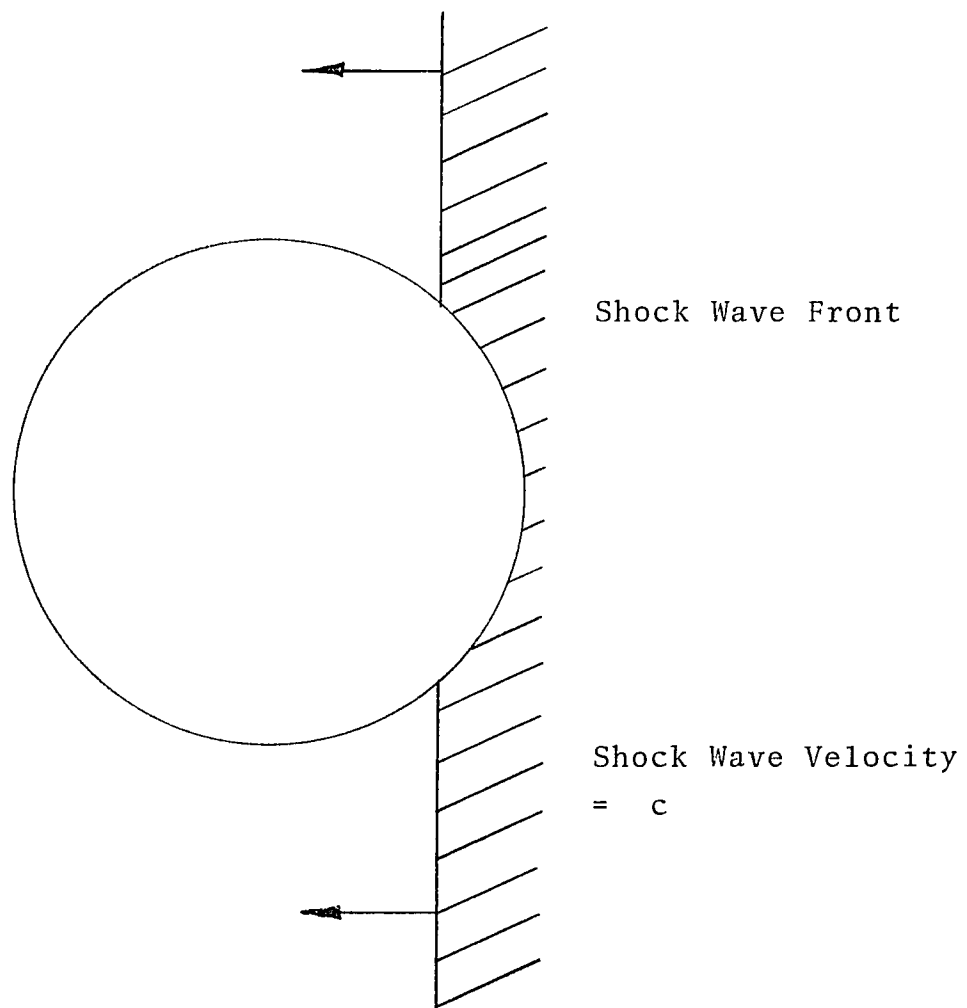


Figure 2.2 - Shock Wave Movement

## CHAPTER 3

ENERGY OF THE STIFFENED STRUCTURE

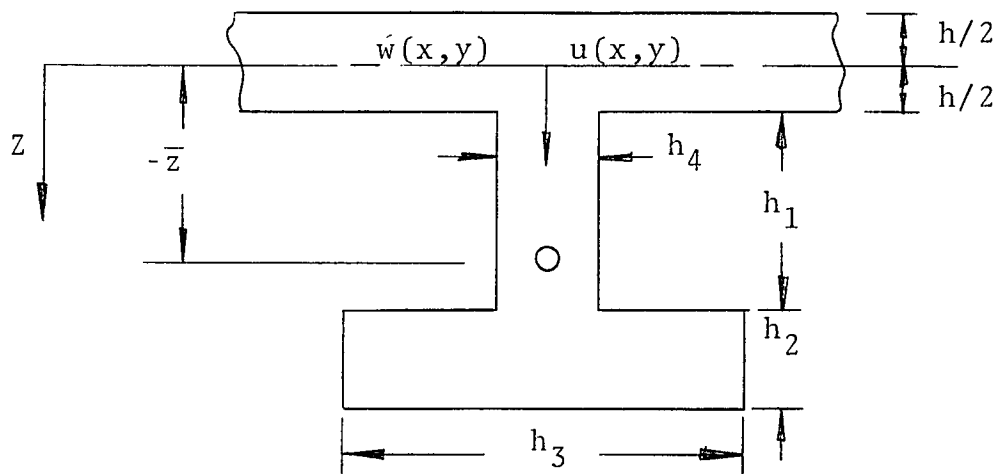
Consider an axisymmetric structure consisting of a cylindrical shell with a reinforcing stiffener. In the cylindrical portion of the structure, the displacements of the shell are defined by the three orthogonal components  $u$ ,  $v$ ,  $w$ , which are functions of the coordinates  $x$  and  $y$  (see Figure 2.1). The stiffener displacements  $u$ ,  $v$ ,  $w$ , are shown in Figure 3.1, where  $h$  is the thickness of the cylindrical shell.

Potential Energy

The strain energy of the unstiffened thin-walled isotropic cylinder [12] is

$$V_c = \frac{E}{2(1-\mu^2)} \int_{-\frac{h}{2}}^{\frac{h}{2}} \int_0^{2\pi R} \int_0^a \left( \epsilon_{xT}^2 + \epsilon_{yT}^2 + 2\epsilon_{xT}\epsilon_{yT} + \frac{1-\mu}{2} \gamma_{xyT}^2 \right) dx dy dz \quad (3.1)$$

in which  $\epsilon_{xT}$ ,  $\epsilon_{yT}$  and  $\gamma_{xyT}$  are the total normal and shearing strains,  $E$  is Young's modulus, and  $\mu$  is Poisson's ratio. When the thickness  $h$  is sufficiently small compared to the radius  $R$ , the cylinder is considered to be a thin-walled cylinder.



○ Stiffener Centroid

Figure 3.1 - Stiffener Geometry

The Donnell type nonlinear strain displacement relations used here are

$$\begin{aligned}\epsilon_{xT} &= u_{T,x} + \frac{1}{2} w_{,x}^2 \\ \epsilon_{yT} &= v_{T,y} + w/R + \frac{1}{2} w_{,y}^2 \\ \gamma_{xyT} &= u_{T,y} + v_{T,x} + w_{,x} w_{,y}\end{aligned}\quad (3.2)$$

where

$$\begin{aligned}u_T &= u - zw_{,x} \\ v_T &= v - zw_{,y}\end{aligned}\quad (3.3)$$

The quantities  $u, v$ , and  $w$  are the displacements of the middle surface of the cylinder wall. Thus,

$$\begin{aligned}\epsilon_{xT} &= u_{,x} + \frac{1}{2} w_{,x}^2 - zw_{,xx} \\ \epsilon_{yT} &= v_{,y} + \frac{w}{R} + \frac{1}{2} w_{,y}^2 - zw_{,yy} \\ \gamma_{xyT} &= u_{,y} + v_{,x} + w_{,x} - 2zw_{,xy}\end{aligned}\quad (3.4)$$

After integration with respect to  $z$ , the cylinder strain energy becomes

$$\begin{aligned}
V_c = & \frac{Eh}{2(1-\mu^2)} \int_0^{2\pi R} \int_0^a \left( \epsilon_x^2 + \epsilon_y^2 + 2\mu\epsilon_x\epsilon_y + \frac{1-\mu}{2} \gamma_{xy}^2 \right) dx dy \\
& + \frac{D}{2} \int_0^{2\pi R} \int_0^a \left[ w_{,xx}^2 + w_{,yy}^2 - 2\mu w_{,xx} w_{,yy} \right. \\
& \left. + 2(1-\mu) w_{,xy}^2 \right] dx dy \quad (3.5)
\end{aligned}$$

where

$$\begin{aligned}
\epsilon_x &= \epsilon_{xT} \Big|_{z=0} \\
\epsilon_y &= \epsilon_{yT} \Big|_{z=0} \\
\gamma_{xy} &= \gamma_{xyT} \Big|_{z=0} \quad (3.6)
\end{aligned}$$

If the displacement in the cylinder and stiffening rings are continuous and the properties of the stiffening rings are averaged over the spacing  $\lambda$ , the total strain energy [12] for the stiffening rings of spacing  $\lambda$  attached to the shell is found to be

$$\begin{aligned}
 V_r = & \frac{1}{l} \int_0^{2\pi R} \left( \frac{E_r}{2} \int_0^a \int_{A_r} \varepsilon_{xT}^2 dA_r dx + \right. \\
 & \left. \frac{G_r J_r}{2} \int_0^a w_{,xy}^2 dx \right) dy \quad (3.7)
 \end{aligned}$$

The first term in equation (3.7) is the strain energy of extension and bending. The quantity  $dA_r$  is an element of cross-sectional area of the stiffening ring, and  $G_r J_r$  is the twisting stiffness of the ring section. Substitution of the first of the equations (3.4) into equation (3.7) and integrating over the area of the stiffening ring yields the following expression for the stiffening ring strain energy

$$\begin{aligned}
 V_r = & \frac{1}{l} \int_0^{2\pi R} \int_0^a \left[ \frac{E_r}{2} \left( A_r \varepsilon_y^2 - 2\bar{z}_r A_r \varepsilon_y w_{,yy} + \right. \right. \\
 & \left. \left. I_{or} w_{,yy} \right) + \frac{G_r J_r}{2} w_{,xy}^2 \right] dx dy \quad [3.8]
 \end{aligned}$$



Here  $\bar{z}_r$  is the distance from the middle surface of the isotropic shell to the centroid of ring cross-section, and  $I_{or}$  is the moment of inertia of the stiffening ring with respect to an axis in the middle surface of the isotropic shell. It should be noted that  $\bar{z}_r$  is positive for a stiffening ring on the outer surface of the shell and negative for a ring on the inner surface.

The potential energy of external pressure and an externally applied axial load resultant  $\bar{N}_x$  (positive in compression) is

$$V_P = \int_0^{2\pi R} \int_0^a P w dx dy + \int_0^{2\pi R} \left[ \bar{N}_x \quad u_T |_{z = \bar{e}} \right] \Big|_0^L dy$$

(3.9)

where

$\bar{N}_x$  = function of  $P_h$  in this case

$P = P_h + P_i = P_r$

$P_h$  = constant external pressure

$P_i$  = incident pressure

$P_r$  = radiated pressure

The quantity  $\bar{e}$  is the distance from the middle surface of the isotropic shell to the line on which the load resultant  $\bar{N}_x$  acts.

The potential strain energy of the combined structure can be written as the sum of the energies of the cylindrical shell, the stiffening rings, and the loads as follows:

$$V = V_c + V_r + V_p \quad (3.10)$$

### Kinetic Energy

The kinetic energy of the system can be written in terms of the kinetic energies of the cylindrical shell segments and the stiffening rings.

The kinetic energy of the unstiffened thin-walled cylinder is

$$T_c = \frac{1}{2} \int_0^L \int_0^{2\pi R} \rho_c h (\dot{u}^2 + \dot{v}^2 + \dot{w}^2) dx dy \quad (3.11)$$

in which  $\rho_c$  is the density of cylinder material.

The kinetic energy of the stiffening ring is

$$T_r = \frac{1}{2} \int_0^L \int_0^{2\pi R} \rho_r \frac{A_r}{l} (\dot{u}^2 + \dot{v}^2 + \dot{w}^2) dx dy \quad (3.12)$$

in which  $\rho_r$  is the density of ring material.

The total kinetic energy of the system is

$$T = \frac{1}{2} \int_0^L \int_0^{2\pi R} \bar{M} (\dot{u}^2 + \dot{v}^2 + \dot{w}^2) dx dy \quad (3.13)$$

where

$$\bar{M} = \rho_c h + \rho_r \frac{A_r}{l} \quad (3.14)$$

is the average or distributed mass per unit area.

## CHAPTER 4

EQUATION DERIVATION & NUMERICAL RESULTSEquation of Motion and Boundary Conditions

The partial differential equations and boundary conditions are derived from Hamilton's principle

$$\delta \int_{t_1}^{t_2} [T - V] dt = 0 \quad (4.1)$$

where  $T$  and  $V$  are the structural system's kinetic energy and potential energy respectively.

The three motions of this conservative system from a given initial configuration to a given final configuration in a time interval  $(t_1, t_2)$  are obtained by allowing variation of the three displacements  $\delta u$ ,  $\delta v$  and  $\delta w$  to be arbitrary and utilizing the fundamental technique of the calculus of variations [13]. From equation (4.1), the three equations of motion are derived as follows:

$$\begin{aligned}
& u_{,xx} + \frac{\mu}{R} w_{,x} + \frac{1-\mu}{2} (u_{,xy} + w_{,x} w_{,xy}) \\
& + \frac{1+\mu}{2} (v_{,xy} + w_{,y} w_{,xy}) - \bar{M}\ddot{u} = 0
\end{aligned}$$

$$\begin{aligned}
& 1 + \left[ \frac{E_r A_r}{Eh\bar{l}} (1-\mu^2) \right] (v_{,xx} + \frac{1}{R} w_{,y} + w_{,y} w_{,yy}) \\
& + \frac{1+\mu}{2} (u_{,xy} + w_{,x} w_{,xy}) + \frac{1-\mu}{2} (v_{,xy} + w_{,xx} w_{,y}) \\
& - \frac{E_r A_r}{Eh\bar{l}} (1-\mu^2) \bar{z}_r w_{,yy} - \bar{M}\ddot{v} = 0
\end{aligned}$$

$$\begin{aligned}
D\nabla^4 w + \frac{1}{R} \left( \frac{Eh}{1-\mu^2} + \frac{E_r A_r}{\bar{l}} \right) (v_{,y} + \frac{w}{R} + \frac{1}{2} w_{,y}^2) \\
+ \frac{E_r}{\bar{l}} (I_r + \frac{\bar{z}_r^2}{\bar{l}} A_r) w_{,yyyy} - \frac{\bar{z}_r E_r A_r}{\bar{l}} (v_{,yyyy} \\
+ \frac{2}{R} w_{,yy} + w_{,yy} + w_{,y} w_{,yyy}) + \\
+ \frac{Eh}{(1-\mu^2)R} (u_{,x} + \frac{1}{2} w_{,x})
\end{aligned}$$

$$\begin{aligned}
& + \frac{Eh}{1-\mu^2} \left[ u_{,x} + \frac{1}{2} w_{,x}^2 + \mu \left( v_{,y} + \frac{w}{R} + \frac{1}{2} w_{,y} \right) \right] w_{,xx} \\
& - \frac{Eh}{1-\mu^2} \left[ v_{,y} + \frac{w}{R} + \frac{1}{2} w_{,y}^2 + \mu u_{,x} + \frac{1}{2} w_{,x}^2 \right] w_{,yy} \\
& - \frac{E_r A_r}{l} \left( v_{,y} + \frac{w}{R} + \frac{1}{2} w_{,x} - \bar{z}_r w_{,yy} \right) w_{,yy} \\
& - 2 \frac{Eh}{2(1+\mu)} \left( v_{,y} + v_{,x} w_{,x} w_{,y} \right) w_{,xy} - \bar{M} \ddot{w} = 0 \quad (4.2)
\end{aligned}$$

The necessary and sufficient conditions to cause the equation (4.1) to vanish during the variational process (3.1) are to zero the remainder part in addition to the equation of motions. Then the natural boundary conditions are established. These conditions at each end of the stiffened cylindrical shell are:

$$\begin{aligned}
& D \left[ w_{,xxx} + (2-\mu) w_{,xyy} \right] - \frac{Eh}{1-\mu^2} \left[ u_{,x} + \frac{1}{2} w_{,x}^2 \right. \\
& + \left. \mu \left( v_{,y} + \frac{w}{R} + w_{,x}^2 \right) \right] w_{,x} - \frac{Eh}{2(1+\mu)} (u_{,y} + v_{,x} \\
& + w_{,x} w_{,y}) w_{,y} = 0
\end{aligned}$$

$$\text{or } w = 0$$

$$D \left( w_{,xx} + \mu w_{,yy} \right) - \bar{N}_x \bar{e} = 0$$

$$\text{or } w_{,x} = 0$$

$$\frac{Et}{1-\mu^2} \left[ u_{,x} + \frac{1}{2} w_{,x}^2 + \mu \left( v_{,y} + \frac{w}{R} + \frac{1}{2} w_{,y}^2 \right) \right]$$

$$+ \bar{N}_x = 0$$

$$\text{or } u = 0$$

$$Gt \left( u_{,y} + v_{,x} + w_{,x} w_{,y} \right) = 0$$

$$\text{or } v = 0$$

(4.3)

Equations (4.2) may be conveniently rewritten in terms of the stress resultants as



$$\begin{aligned}
N_{x,x} + N_{xy,y} - \bar{M}\ddot{u} &= 0 \\
N_{y,y} + N_{xy,x} - \bar{M}\ddot{v} &= 0 \\
-M_{x,xx} + M_{xy,xy} - M_{yx,xy} - M_{y,yy} + \frac{N_y}{R} \\
&- N_x w_{,xx} - N_y w_{,yy} - 2N_{xy} w_{,xy} + P - \bar{M}\ddot{w} \\
&= 0 \tag{4.4}
\end{aligned}$$

The boundary conditions (4.3) may be rewritten in terms of stress resultants as

$$M_{x,x} - (M_{xy,y} - M_{yx,y}) + N_x w_{,x} + N_{xy} w_{,y} = 0$$

$$\text{or } w = 0$$

$$M_x + \bar{N}_x \bar{e} = 0$$

$$\text{or } w_{,x} = 0$$

$$N_x + \bar{N}_x = 0$$

$$\text{or } u = 0$$

$$N_{xy} = 0$$

$$\text{or } v = 0$$

(4.5)

where

$$N_x = \frac{Eh}{1-\mu^2} \left[ u_{,x} + \frac{1}{2} w_{,x}^2 + \mu \left( v_{,y} + \frac{w}{R} + \frac{1}{2} w_{,y}^2 \right) \right]$$

$$N_y = \frac{Eh}{1-\mu^2} \left[ v_{,y} + \frac{w}{R} + \frac{1}{2} w_{,y}^2 + \mu \left( u_{,x} + \frac{1}{2} w_{,x}^2 \right) \right]$$

$$+ \frac{E_r A_r}{l} \left( v_{,y} + \frac{w}{R} + \frac{1}{2} w_{,y}^2 - \bar{z}_r w_{,yy} \right)$$

$$N_{xy} = Gh \left( v_{,y} + v_{,x} + w_{,x} w_{,y} \right)$$

$$M_x = -D \left( w_{,xx} + \mu w_{,yy} \right)$$

$$M_y = -D \left( w_{,yy} + \mu w_{,xx} \right) - \frac{E_r I_r}{l} w_{,yy} \\ + \bar{z}_r \frac{E_r A_r}{l} \left( v_{,y} + \frac{w}{R} - \frac{1}{2} w_{,y}^2 - \bar{z}_r w_{,yy} \right)$$

$$M_{xy} = \frac{Gh}{6} w_{,xy}$$

$$M_{yx} = -\left(\frac{Gh}{6} + \frac{G_r J_r}{l}\right) w_{,xy} \quad (4.6)$$

### Vibration Equations

The equations of motion (4.4) derived in the last section are used to obtain linear equations which govern the small amplitude vibrations of a prestressed, eccentrically stiffened, cylindrical shell which is submerged in a fluid medium.

The deformations associated with the vibration of a prestressed cylinder are divided into two parts as follows:

$$u = u_A + u_B$$

$$v = v_A + v_B$$

$$w = w_A + w_B \quad (4.7)$$

The first part, denoted by subscript A, is an axisymmetric static prestress deformation which occurs prior to excitation at one of the natural frequencies. The second part, denoted

by subscript B, is a small additional deformation which occurs as a result of the excitation. Since the A subscripted quantities are static they are axisymmetric deformations; therefore, the terms  $\bar{M}\ddot{u}_A$ ,  $\bar{M}\ddot{v}_A$ ,  $\bar{M}\ddot{w}_A$  and all derivatives with respect to  $y$  vanish. The equilibrium equations which govern these deformations are found from equations (4.4) as

$$N_{xA,x} = 0$$

$$N_{xyA,x} = 0$$

$$-M_{xA,xx} + \frac{N_{yA}}{R} - N_{xA}w_{A,xx} + (p_h + p_i) = 0 \quad (4.8)$$

If there is no applied shear, equation (4.8) yields

$$N_{xyA} = 0$$

If we let all derivatives with respect to  $y$  equal zero for axisymmetric deformation, a set of appropriate boundary conditions are found from equations (4.5) to be

$$M_{xA,x} + N_{xA} w_A = 0$$

$$\text{or } w_A = 0$$

$$M_{xA} + \bar{N}_x \bar{e} = 0$$

$$\text{or } w_{A,x} = 0$$

$$N_{xA} + \bar{N}_x = 0$$

$$\text{or } u_A = 0$$

$$N_{xyA} = 0$$

$$\text{or } v_A = 0$$

where

$$N_{xA} = \frac{Et}{1-\mu^2} \left[ u_{A,x} + \frac{1}{2} w_{A,x}^2 + \mu \left( -\frac{w_A}{R} \right) \right]$$

$$N_{yA} = \frac{Et}{1-\nu^2} \left[ \frac{w_A}{R} + \left( u_{A,x} + \frac{1}{2} w_{A,x}^2 \right) \right] + \frac{E_r A_r}{l} \frac{w_A}{R}$$

$$N_{xyA} = G w_{A,x}$$

$$M_{xA} = -D w_{A,xx}$$

The equilibrium equations and boundary conditions which govern the dynamic deformations (subscript B) are obtained by substituting equation (4.7) into equation (4.4) and (4.5). By eliminating the axisymmetric pre-stress equations, and retaining only linear terms, i.e. neglecting the high order terms under the small amplitude vibration assumption, the following equations governing the dynamic deformations (subscript B) are obtained:

$$N_{xB,x} + N_{xyB,y} - \bar{M}\ddot{u}_B = 0$$

$$N_{yB,y} + N_{xyB,x} - M\ddot{v}_B = 0$$

$$\begin{aligned}
& - M_{xB,xx} + M_{xyB,xy} - M_{yxB,xy} - M_{yB,yy} \\
& + \frac{N_{yB}}{R} - N_{xA} w_{B,xx} - N_{xB} w_{A,xx} - N_{yA} w_{B,yy} \\
& + P_r - \bar{M} \ddot{w}_B = 0 \tag{4.11}
\end{aligned}$$

and the boundary conditions become

$$\begin{aligned}
M_{xB,x} - (M_{xyB,y} - M_{yxb,y}) + N_{xA} w_{B,x} \\
+ N_{xB} w_{A,x} = 0
\end{aligned}$$

$$\text{or } w_B = 0$$

$$M_{xB} = 0$$

$$\text{or } w_{B,x} = 0$$

$$N_{xB} = 0$$

$$\text{or } u_B = 0$$

$$N_{xyB} = 0$$

$$\text{or } v_B = 0 \quad (4.12)$$

where

$$N_{xB} = \frac{Et}{1-\mu^2} \left[ u_{B,x} + w_{A,x} w_{B,x} + \mu \left( v_{B,y} + \frac{w_B}{R} \right) \right]$$

$$N_{yB} = \frac{Et}{1-\mu^2} \left[ v_{B,y} + \frac{w_B}{R} + \mu \left( u_{B,x} + w_{A,x} w_{B,x} \right) \right]$$

$$+ \frac{E_r A_r}{l} \left( v_{B,y} + \frac{w_B}{R} - \bar{z}_r w_{B,yy} \right)$$

$$N_{xyB} = Gh \left( u_{B,x} + v_{B,x} + w_{A,x} w_{B,y} \right)$$

$$M_{xB} = -D \left( w_{B,xx} + \mu w_{B,yy} \right)$$



$$M_{yB} = -D \left( w_{B,yy} + \mu w_{B,xx} \right) - \frac{E_r I_r}{l} w_{B,yy} \\ + \bar{z}_r \frac{E_r A_r}{l} \left( v_{B,y} + \frac{w_B}{R} - \bar{z}_r w_{B,yy} \right)$$

$$M_{xyB} = \frac{Gh}{6} w_{B,xy}$$

$$M_{yxB} = - \left( \frac{Gh}{6} + \frac{G_r J_r}{l} \right) w_{B,xy} \quad (4.13)$$

### Frequency Equation Derivation

Assuming a constant prestress deformation  $w_A$ , the solution equations are

$$N_{xA} = - \bar{N}_x = - \frac{PR}{2}$$

$$N_{yA} = - \bar{N}_y = - PR \quad (4.14)$$

Equation (4.11) may now be written as

$$N_{xB,x} + N_{xyB,y} - \bar{M} \ddot{u}_B = 0$$

$$N_{yB,y} + N_{xyB,x} - \bar{M} \ddot{v}_B = 0$$

$$- M_{xB,xx} + M_{xyB,xy} - M_{yxB,xy} - M_{yB,yy}$$

$$+ \frac{N_{yB}}{R} + \bar{N}_x w_{B,xx} + \bar{N}_y w_{B,yy} + P_r$$

$$- \bar{M} \ddot{w}_B = 0 \quad (4.15)$$

The displacement  $u_B$ ,  $v_B$  and  $w_B$  which satisfy simple support boundary conditions are given as

$$u_B = \bar{U} e^{i\omega t} \cos\left(\frac{m\pi x}{L}\right) \sin\left(\frac{ny}{R}\right)$$

$$v_B = \bar{V} e^{i\omega t} \sin\left(\frac{m\pi x}{L}\right) \sin\left(\frac{ny}{R}\right)$$

$$w_B = \bar{W} e^{i\omega t} \sin\left(\frac{m\pi x}{L}\right) \cos\left(\frac{ny}{R}\right) \quad (4.16)$$

The equation (2.11) gives

$$P_r = \rho_w \omega^2 f(\omega) e^{i\omega t} \bar{W} \sin\left(\frac{m\pi x}{L}\right) \cos\left(\frac{ny}{R}\right)$$

where  $m$  is the number of axial half-waves and  $n$  is the number of circumferential full waves. If equations (4.16) are substituted into equation (4.15) it yields

$$\begin{aligned} & - \left( M\omega^2 + \frac{Eh}{1-\mu^2} \frac{m^2\pi^2}{L} + Gh \frac{n^2}{R} \right) \bar{U} \\ & + \frac{mn\pi}{LR} \left( \frac{\mu Eh}{1-\mu} + Gh \right) \bar{V} - \frac{\mu Eh}{1-\mu^2} \frac{m\pi}{LR} \bar{W} = 0 \end{aligned}$$

$$\begin{aligned} & \frac{mn\pi}{LR} \left( \frac{\mu Eh}{1-\mu} + Gh \right) \bar{U} - \left( \bar{M}\omega^2 + \frac{Eh}{1-\mu^2} \frac{n^2}{R^2} \right. \\ & \quad \left. + \frac{E_r A_r}{l} \frac{n^2}{R^2} + Gh \frac{m^2\pi^2}{L^2} \right) \bar{V} - \frac{n}{R^2} \left( \frac{Eh}{1-\mu^2} \right. \\ & \quad \left. + \frac{E_r A_r}{l} + \frac{E_r A_r z_r n^2}{lR} \right) \bar{W} = 0 \end{aligned}$$

$$\begin{aligned}
& \frac{\mu E h}{1-\mu^2} \frac{\mu m \pi}{R L} \bar{U} - \frac{n}{R^2} \left( \frac{E h}{1-\mu^2} + \frac{E_r A_r}{l} \right. \\
& \left. + \frac{E_r A_r z_r^n}{l R} \right) \bar{V} - \left[ D \left[ \left( \frac{m \pi}{L} \right)^4 + \left( \frac{n}{R} \right)^4 + 2 \mu \left( \frac{m n}{L R} \right)^2 \right] \right. \\
& \left. + \left( \frac{G h^3}{3} + \frac{G_r J_r}{l} \right) \left( \frac{m n \pi}{L R} \right)^2 + \frac{E_r I_r}{l} \left( \frac{n}{R} \right)^4 \right. \\
& \left. + \frac{E_r A_r}{l R^2} \left[ 1 + \bar{z}_r \left( \frac{2 n}{R} \right)^2 + \bar{z}_r \frac{n^4}{R^2} \right] + \frac{E h}{1-\mu^2} \frac{1}{R^2} \right. \\
& \left. - \bar{N}_x \left( \frac{m \pi}{L} \right)^2 - \bar{N}_y \left( \frac{n}{R} \right)^2 - \left[ \bar{M} + \rho_w f(\omega) \right] \omega^2 \right] \bar{W} = 0
\end{aligned}
\tag{4.17}$$

The determinant of the displacement coefficients when set equal to zero yields a sixth-order equation of the circular frequency.

$$[A] = 0 \tag{4.18}$$

where

$$A_{12} = A_{21} = \frac{m n \pi}{L R} \left( G h + \frac{\mu E h}{1-\mu^2} \right)$$

$$\begin{aligned}
A_{13} &= A_{31} = \frac{\mu E h}{1 - \mu^2} \frac{m \pi}{LR} \\
A_{23} &= A_{32} = - \frac{n}{R^2} \left[ \frac{E h}{1 - \mu^2} + \frac{E_r A_r}{l} \left( 1 + \bar{z}_r \frac{n^2}{R^2} \right) \right] \\
A_{11} &= - \left( \bar{M} \omega^2 + \frac{E h}{1 - \mu^2} \frac{m^2 \pi^2}{L^2} + G h \frac{n^2}{R^2} \right) \\
A_{22} &= - \left( \bar{M} \omega^2 + \frac{E h}{1 - \mu^2} \frac{n^2}{R^2} + \frac{E_r A_r}{l} \frac{n^2}{R^2} + G h \frac{m^2 \pi^2}{L^2} \right) \\
A_{33} &= \left[ \bar{M} + \rho_w f(\omega) \right] \omega^2 - \left[ D \left[ \left( \frac{m \pi}{L} \right)^4 + \left( \frac{n}{R} \right)^4 + 2 \mu \left( \frac{m n}{LR} \right)^2 \right] \right. \\
&\quad + \left( \frac{G h^3}{3} + \frac{G_r J_r}{l} \right) \left( \frac{m n \pi}{LR} \right)^2 + \frac{E_r J_r}{l} \left( \frac{n}{R} \right)^4 \\
&\quad + \frac{E_r A_r}{l R^2} \left[ 1 + \bar{z}_r \left( \frac{2 n^2}{R} + \bar{z}_r \frac{n^4}{R^2} \right) \right] \\
&\quad \left. + \frac{E h}{1 - \mu^2} \frac{1}{R^2} - \bar{N}_x \left( \frac{m \pi}{L} \right)^2 - \bar{N}_y \left( \frac{n}{R} \right)^2 \right] \quad (4.19)
\end{aligned}$$

The result of  $[A] = 0$  is

$$\Lambda_3 \omega^6 + \Lambda_2 \omega^4 + \Lambda_1 \omega^2 + \Lambda_0 = 0 \quad (4.20)$$

where

$$F_1 = \left[ \bar{M} + \rho_w F(\omega) \right]$$

$$F_2 = \frac{Eh}{1-\mu^2} \frac{m^2 \pi^2}{L^2} + Gh \frac{n^2}{R^2}$$

$$F_3 = \left( \frac{Eh}{1-\mu^2} + \frac{E_r A_r}{l} \right) \frac{n^2}{R^2} + Gh \frac{m^2 \pi^2}{L^2}$$

$$F_4 = A_{12} = \left( Gh + \mu \frac{Eh}{1-\mu^2} \right) \frac{mn\pi}{LR}$$

$$F_5 = A_{23} = - \left[ \frac{Eh}{1-\mu^2} + \frac{E_r A_r}{l} \left( 1 + \bar{z}_r \frac{n^2}{R} \right) \right] \frac{n}{R^2}$$

$$F_6 = A_{13} = \frac{\mu Eh}{1-\mu^2} \frac{m\pi}{LR}$$

$$\begin{aligned}
F_7 = & D \left[ \left( \frac{m\pi}{L} \right)^4 + \left( \frac{n}{R} \right)^4 + 2\mu \left( \frac{mn\pi}{LR} \right)^2 \right] \\
& + \left( \frac{Gh^3}{3} + \frac{G_r J_r}{I} \right) \left( \frac{mn\pi}{LR} \right)^2 + \frac{E_r I_r}{I} \left( \frac{n}{R} \right)^4 \\
& + \frac{E_r A_r}{I R^2} \left[ 1 + \bar{z}_r \left( \frac{2n^2}{R} + \bar{z}_r \frac{n^4}{R^2} \right) \right] \\
& + \frac{Eh}{1-\mu^2} \frac{1}{R^2} - \bar{N}_x \left( \frac{m\pi}{L} \right)^2 - \bar{N}_y \left( \frac{n}{R} \right)^2
\end{aligned} \tag{4.21}$$

and

$$\begin{aligned}
\Lambda_3 &= F_1 \bar{M}^2 \\
\Lambda_2 &= \bar{M} \left[ F_1 (F_2 + F_3) - \bar{M} F_7 \right] \\
\Lambda_1 &= F_1 \left[ F_2 F_3 - (F_4)^2 \right] - \bar{M} \left[ (F_2 + F_3) F_7 - (F_5)^2 - (F_6)^2 \right] \\
\Lambda_0 &= \left[ (F_4)^2 - F_2 F_3 \right] F_7 + (F_5)^2 F_2 + (F_6)^2 F_3 \\
&+ 2F_4 F_5 F_6
\end{aligned} \tag{4.22}$$

### Mode Separation

It is convenient to write the system of equations (4.17) in matrix form

$$[A] [D] = 0$$

where  $[D]$  is the vector  $\begin{bmatrix} \bar{U} \\ \bar{V} \\ \bar{W} \end{bmatrix}$  (4.23)

The natural frequency,  $\omega$ , is obtained by equating the determinant  $[A]$  to zero. Substituting the value of  $\omega$  into equation (4.23), the non-trivial solution will provide the amplitude ratios from the three algebraic equations of the coefficients of  $\bar{U}$ ,  $\bar{V}$  and  $\bar{W}$ .



### Numerical Procedures

The solution of the frequency equation (4.20) involves modified Bessel functions. These functions were evaluated by the IBM computer subroutine program BESK, which computes the zero-order and first-order Bessel functions using series approximations and then computes the high-order function using the recurrence relation [14]. The accuracy was checked by comparing it with published data [14]. The natural frequencies,  $\omega$ , were obtained by an iterative procedure. The root of the nonlinear frequency equation is computed by subroutine ZEROIN in which the bisection method and secant rule are used [15].

For the consideration of one degree of freedom, only the radial surface motion of the system is permitted and other surface motions are neglected. The frequency equation is derived from equation (4.18) by equating  $\bar{M}\omega^2$  terms to zero in  $A_{11}$  and  $A_{22}$ . This equation has the following form:

$$\Lambda_1' \omega^2 + \Lambda_0' = 0$$

The frequency  $\omega$  is found exactly.

For the purpose of comparing with McElmans' method, the fluid-structure interaction is decoupled from this one degree of freedom frequency equation. Actually, this equation represents another form of the McElman equation.

#### Comparison with McElmans' Method

The design example given in reference [16] was evaluated in vacuum and in seawater at a depth of 1,000 feet. The preassigned parameters were given the values:

$R = 198.0$  in.,  $L = 504.0$  in.,  $h = 1.2056$  in.,  
 $l = 30.17$  in.,  $\mu = 0.33$ ,  $E = 30 \times 10^6$  psi,  
 $\rho_c = 7.33 \times 10^{-4}$  slug/in.,  $\rho_w = 0.97 \times 10^{-4}$  slug/in.,  
 $c = 60,000$  in/sec. (average sound velocity in saltwater),  
 $h_1 = 10.02$  in.,  $h_2 = 0.3071$  in.,  $h_3 = 10.363$  in.,  
 $h_4 = 0.2373$  in. (the stiffener dimension  $h_i$  is shown in Figure 2.1).

The example was evaluated in this study by four different methods as detailed below.

1. McElman's method with prestress which is formed by the pressure associated with a depth of water of 1,000 ft.
2. The present one degree of freedom method with the fluid-structure interaction decoupled.
3. The present one degree of freedom method with fluid-structure interaction.
4. The present three degree of freedom method with fluid structure interaction.

The numerical results are presented in Table I.

The results of methods 1 and 2 are identical. They show that both equations, though of different formulation, are equivalent. The results of method 3 and 4 give much lower natural frequencies when the structure is submerged in water. In these methods, the tangential and axial motion are not significant. The elimination of these two degrees of freedom in method 3 gave only slightly different natural frequencies than in method 4.

Table I - Natural Frequencies (Hz) Comparison with  
McElman's Method

| Axial<br>Half<br>Wave<br>m | Full<br>Wave<br>n | McElman<br>Method | Present Method                      |                         |  |
|----------------------------|-------------------|-------------------|-------------------------------------|-------------------------|--|
|                            |                   |                   | One Degree<br>Freedom<br>Considered |                         | Three Degrees<br>Freedom<br>Considered |
|                            |                   |                   | in Vacuum                           | in Water<br>1000' Depth | in Water<br>1000' Depth                |
| 1                          | 2                 | 30.06             | 30.06                               | 10.68                   | 10.85                                  |
| 1                          | 3                 | 15.17             | 15.17                               | 6.11                    | 6.18                                   |
| 2                          | 4                 | 41.47             | 41.47                               | 18.97                   | 19.11                                  |
| 3                          | 5                 | 66.78             | 66.78                               | 33.78                   | 33.74                                  |

Comparison with Experiments Conducted in Water by Norfolk Naval Shipyard [10]

The tests were conducted by the Under Water Explosion Research Division of the Norfolk Naval Shipyard [10]. Several aspects of the experimental program such as the use of massive bulkheads and extended end sections, were introduced in order to make the experimental model more nearly the match of the cylindrical shell of infinite length, with radial surface motions over only a finite section. The dimensions and characteristics of the ring-stiffened cylinder are :

$$\begin{aligned}
 R &= 20.25 \text{ in.}, \quad L = 60.75 \text{ in.}, \quad h = 0.177 \text{ in.}, \\
 L/l &= 17, \quad E = 30 \times 10^6 \text{ psi}, \quad \mu = 0.3, \\
 \rho_c &= 7.77 \times 10^{-4} \text{ slug/in.}, \quad \rho_w = 0.934 \times 10^{-4} \text{ slug/in.}, \\
 c &= 60,000 \text{ in/sec.}, \quad (\rho A)_{\text{ring}} = 0.25 \times 10^{-5} \text{ lb/sec/in.}, \\
 (EA)_{\text{ring}} &= 9.68 \times 10^6 \text{ lb/in.}, \quad \bar{Z}_r = 0.98 \text{ in.}
 \end{aligned}$$

The above example was evaluated by the present three degree of freedom approach. The numerical results are presented in Table II.

From Table II, it is evident that the natural frequencies calculated by the present method are slightly higher than those obtained in the referenced tests. This result is to be expected since the test model was a long cylinder with radial surface motion over a simply supported section of finite length, whereas the analytical model consisted of only a simply supported cylinder of identical finite length. Thus, the experimental model had a longer "effective" length than the analytical model. Based on elementary beam theory in which the natural frequencies are inversely proportional to the square of the effective length, the tested frequencies should be lower than those predicted by the presented analytical model.

Table II - Natural Frequencies (Hz) Comparison  
with Underwater Test Data

| Axial Half<br>Wave m | Full Wave<br>n | Experiment*<br>in Water | Present Method**<br>(Depth of Water 5 ft) |
|----------------------|----------------|-------------------------|---|
| 1                    | 2              | 128/138                 | 156                                       |
| 1                    | 3              | 204                     | 210                                       |
| 3                    | 4              | 466                     | 554                                       |
| 3                    | 5              | 655                     | 736                                       |

\* Infinite long cylinder with radial motion over finite section.

\*\* Finite length with simply supported ends.

Comparison with Experiments Conducted in Air by  
Hayek and Pallet [17]

The results of the present method have been compared to a set of experimental results which have been obtained at the Ordinance Research Laboratories by Hayek and Pallet, reference [17]. The experiments were conducted on the stiffened cylindrical shell of the following geometry:

$$\begin{aligned}
 R &= 10.2 \text{ in}, & L &= 30.0 \text{ in}, & h &= 0.33 \text{ in}, \\
 l &= 5.0 \text{ in}, & h_1 &= 1.0 \text{ in}, & h_2 &= h_3 = 0 \text{ in}, \\
 h_4 &= 0.375 \text{ in}, & E &= 10^7 \text{ psi}, & \mu &= 0.33 \text{ in}, \\
 \rho_c &= 0.098 \text{ lb/in},
 \end{aligned}$$

The numerical results are presented in Table III.

It can be seen from Table III that as  $n$  increases, the natural frequencies predicted by this method deviate substantially from the experimental values. The mode shape associated with  $n$  cannot be approximated by an overall sinusoidal wave  $m$  and, therefore, the error involved is large. Similar results appear in the other orthotropic approaches documented by Bleich [18], Galletly [19], Wah [20], and Basdekas-Chi [21]; recommendations for improved results are presented in Chapter VII.



Table III - Natural Frequencies (Hz) Comparison  
with Air Test Data

| Half Wave m | Full Wave n | Experiment in Air | Present Method* |
|-------------|-------------|-------------------|-----------------|
| 1           | 2           | 627               | 727             |
| 1           | 3           | 1190              | 1336            |
| 3           | 0           | 3020              | 3019            |
| 1           | 8           | 3728              | 5897            |

\* One degree freedom is considered

### Mode Separation

The mode separation was conducted in the first example problem of this numerical analysis. The design example was evaluated with the interaction of seawater at a depth of 1000 feet. The previously assigned parameters were given in page 41.

The natural frequencies were obtained from the first example of this analysis. Substituting the values of frequency into equation (4.23), the amplitude ratios are found from the three algebraic equations of the coefficients of  $\bar{U}$ ,  $\bar{V}$  and  $\bar{W}$ . The numerical results are presented in Table IV.

Table IV - Mode Separation

| Axial<br>Half<br>Wave<br>m | Full<br>Wave<br>n | Natural<br>Frequency<br>Hz | Ratios of Mode      |                    |                         |
|----------------------------|-------------------|----------------------------|---------------------|--------------------|-------------------------|
|                            |                   |                            | Radial<br>Amplitude | Axial<br>Amplitude | Tangential<br>Amplitude |
| 1                          | 2                 | 10.85                      | 1.0                 | 0.152              | 0.515                   |
| 1                          | 3                 | 6.18                       | 1.0                 | 0.097              | 0.356                   |
| 2                          | 4                 | 19.11                      | 1.0                 | 0.086              | 0.309                   |
| 3                          | 5                 | 33.74                      | 1.0                 | 0.073              | 0.227                   |

CHAPTER 5  
APPROXIMATE SOLUTIONS

Cylindrical Wave Approximation [8, 23]

The acoustic field equation [2.1], is replaced here by Haywood's approximate relation

$$\frac{\partial \phi}{r} = -\frac{1}{c} \frac{\partial \phi}{\partial t} - \frac{\bar{g}_n}{R} \phi \quad [5.1]$$

Where  $\bar{g}_n$  is the after-flow coefficient. The approximation assumes that each ring element of the the shell radiates a cylindrical wave into the surrounding medium.

The solution of equation of motion [4.15], satisfying the shell boundary condition [4.12], and the shell-fluid boundary condition equation [5.1], is given by

$$\begin{aligned} W &= e^{i\omega t} \bar{W} \sin \frac{m\pi x}{L} \cos \frac{ny}{R} \\ U &= e^{i\omega t} \bar{U} \cos \frac{m\pi x}{L} \cos \frac{ny}{R} \\ V &= e^{i\omega t} \bar{V} \sin \frac{m\pi x}{L} \cos \frac{ny}{R} \\ \phi &= e^{i\omega t} \bar{\phi} \sin \frac{m\pi x}{L} \cos \frac{ny}{R} \\ P_r &= e^{i\omega t} \bar{P}_r \sin \frac{m\pi x}{L} \cos \frac{ny}{R} \end{aligned} \quad [5.2]$$

The velocity of the shell and the velocity of the fluid medium are equal at the shell-fluid interface,  $r = R$ , i.e.

$$\frac{\partial W}{\partial t} = \frac{\partial \phi}{\partial r} \quad [5.3]$$

Substituting equation [5.1] and [5.2] into equation [5.3] results in

$$\phi = - \left\{ \frac{\frac{\omega^2}{C}}{\left(\frac{\bar{g}}{R}\right)^2 + \left(\frac{\omega}{C}\right)^2} + i \frac{\frac{\bar{g}}{R} \omega}{\left(\frac{\bar{g}}{R}\right)^2 + \left(\frac{\omega}{C}\right)^2} \right\} W \quad [5.4]$$

The radiated pressure  $P_r$  is defined by the velocity potential of the fluid medium

$$P_r = \rho_w \frac{\partial \phi}{\partial t} \quad [5.5]$$

Substituting equation [5.2] and [5.4] into equation [5.5] results in

$$\bar{P}_r = \rho \omega^2 \left\{ \frac{\frac{\bar{g}_n}{R}}{\left(\frac{\bar{g}_n}{R}\right)^2 + \left(\frac{\omega}{c}\right)^2} - i \frac{\frac{\omega}{c}}{\left(\frac{\bar{g}_n}{R}\right)^2 + \left(\frac{\omega}{c}\right)^2} \right\} \bar{W} \quad [5.6]$$

The structure is excited by a radial harmonic force assumed to be

$$F = e^{i\omega t} \bar{F} \sin \frac{m\pi x}{L} \cos \frac{n y}{R} \quad [5.7]$$

Substituting equations [5.2] and [5.6] into the equation of motion [4.15] and applying the radial harmonic force [5.7], gives the solution for the amplitude  $\bar{U}$ ,  $\bar{V}$ ,  $\bar{W}$  which may be written as

$$\begin{aligned}\bar{U} &= \bar{F} \quad UU \left[ \frac{\Delta_r}{(\Delta_r)^2 + (\Delta_i)^2} + i \frac{\Delta_i}{(\Delta_r)^2 + (\Delta_i)^2} \right] \\ \bar{V} &= \bar{F} \quad VV \left[ \frac{\Delta_r}{(\Delta_r)^2 + (\Delta_i)^2} + i \frac{\Delta_i}{(\Delta_r)^2 + (\Delta_i)^2} \right] \\ \bar{W} &= \bar{F} \quad WW \left[ \frac{\Delta_r}{(\Delta_r)^2 + (\Delta_i)^2} + i \frac{\Delta_i}{(\Delta_r)^2 + (\Delta_i)^2} \right]\end{aligned}\quad [5.8]$$

where

$$\begin{aligned}\Delta_r &= a_{11} a_{22} a_{33} + 2 A_{12} A_{23} A_{13} - a_{22} (A_{13})^2 \\ &\quad - a_{11} (A_{13})^2 - a_{33} (A_{12})^2\end{aligned}$$

$$\Delta_i = [a_{11} a_{22} - (A_{12})^2] \left\{ \frac{\frac{\omega^3}{c}}{\left(\frac{\bar{g}_n}{R}\right)^2 + \left(\frac{\omega}{c}\right)^2} \right\}$$

$$UU = A_{12} \times A_{23} - a_{22} A_{13}$$

$$VV = A_{13} \times A_{12} - a_{11} A_{23}$$

$$WW = a_{11} a_{22} - (A_{12})^2 \quad [5.9]$$

The  $A_{ij}$  is defined by equation [4.19] and  $a_{ii}$  are given by

$$a_{11} = A_{11} + \bar{M}\omega^2$$

$$a_{22} = A_{22} + \bar{M}\omega^2$$

$$a_{33} = A_{33} - [\bar{M} + \rho \omega f(\omega)] + \rho \frac{\bar{g}_0}{R} \frac{\omega^2}{\frac{\bar{g}_0^2}{R} + \frac{\omega^2}{C^2}} \quad [5.10]$$

Assuming the forcing function to be  $\sin\omega t$ , the imaginary part is only under consideration. Therefore, the resultant amplitude is

$$A(\omega) = \frac{\bar{F}\Delta_i}{\Delta_r^2 + \Delta_i^2} \left( (UU)^2 + (VV)^2 + (WW)^2 \right) \quad [5.11]$$

The maximum  $A(\omega)$  occurs at resonance frequency which is determined numerically.

#### Plane Wave Approximation [ 23 ]

The acoustic field equation is approximated by the relation

$$\frac{\partial \phi}{\partial r} = - \frac{1}{C} \frac{\partial \phi}{\partial t} \quad [5.12]$$

The approximation assumes that each element of the shell radiates a plane wave into the surrounding medium, an assumption which increases in error as the interaction progresses.

Substituting [5.12] and [5.5] into equation [5.3] results in

$$\Phi = - c\bar{W} \quad [5.13]$$

The substitution of equation [5.2] and [5.13] into equation [5.5] leads to

$$\bar{P}_r = - i\rho c\omega\bar{W} \quad [5.14]$$

By the same procedure used in the cylindrical wave approximation method, the resultant amplitude results in

$$A(\omega) = \frac{F \Delta_i}{\Delta_r^2 + \Delta_i^2} \left[ (UU)^2 + (VV)^2 + (WW)^2 \right] \quad [5.15]$$

the  $\Delta_i$  and  $a_{33}$  are redefined as

$$\Delta_i = [a_{11} a_{22} - (A_{12})^2] [\rho c\omega]$$

$$a_{33} = A_{33} - [\bar{M} + \rho\omega f(\omega)]$$

The maximum  $A(\omega)$  occurs at resonance frequency which is determined numerically.



### Parametric Study

A parametric study was conducted for a cylindrical shell submerged in seawater, using the preassigned dimensions listed on page 41, with  $\frac{L}{Rm}$  as the variable. The after-flow coefficients  $\bar{g}_n$  which yield maximum amplitudes (equation 5.11) at the natural frequencies calculated in Chapter 4 are determined numerically and plotted on Figure 5.1. These after-flow coefficients ( $\bar{g}_n$ ) approach the upper bound of Haywood's values [23].

The formula that evolved for the after-flow coefficients is:

$$\bar{g}_n = (\bar{g}_n)_\infty + 9e^{-(3.4 + 0.3n) \left(\frac{L}{Rm} - 0.25\right)}$$

where

$$\begin{array}{ll} (\bar{g}_1)_\infty = 1.43 & (\bar{g}_4)_\infty = 4.24 \\ (\bar{g}_2)_\infty = 2.40 & (\bar{g}_5)_\infty = 5.10 \\ (\bar{g}_3)_\infty = 3.30 & (\bar{g}_6)_\infty = 6.00 \end{array}$$

With these values of  $\bar{g}_n$  it is possible to calculate the natural frequency numerically by the cylindrical wave approximation method.

The accuracy of the plane wave approximate equation [5.15] depends upon the value of  $\rho c$ . For values at  $\rho c$  between

zero and  $60,000 \times 0.97 \times 10^{-4} = 5.82$  slug/sec, it gives agreement only at low values of  $\rho c$ . At  $\rho c = 5.82$  slug/sec the accuracy of the natural frequency is very poor (about 5% to 20%). Therefore, the plane wave approximation is not recommended when the shell is submerged in a fluid.

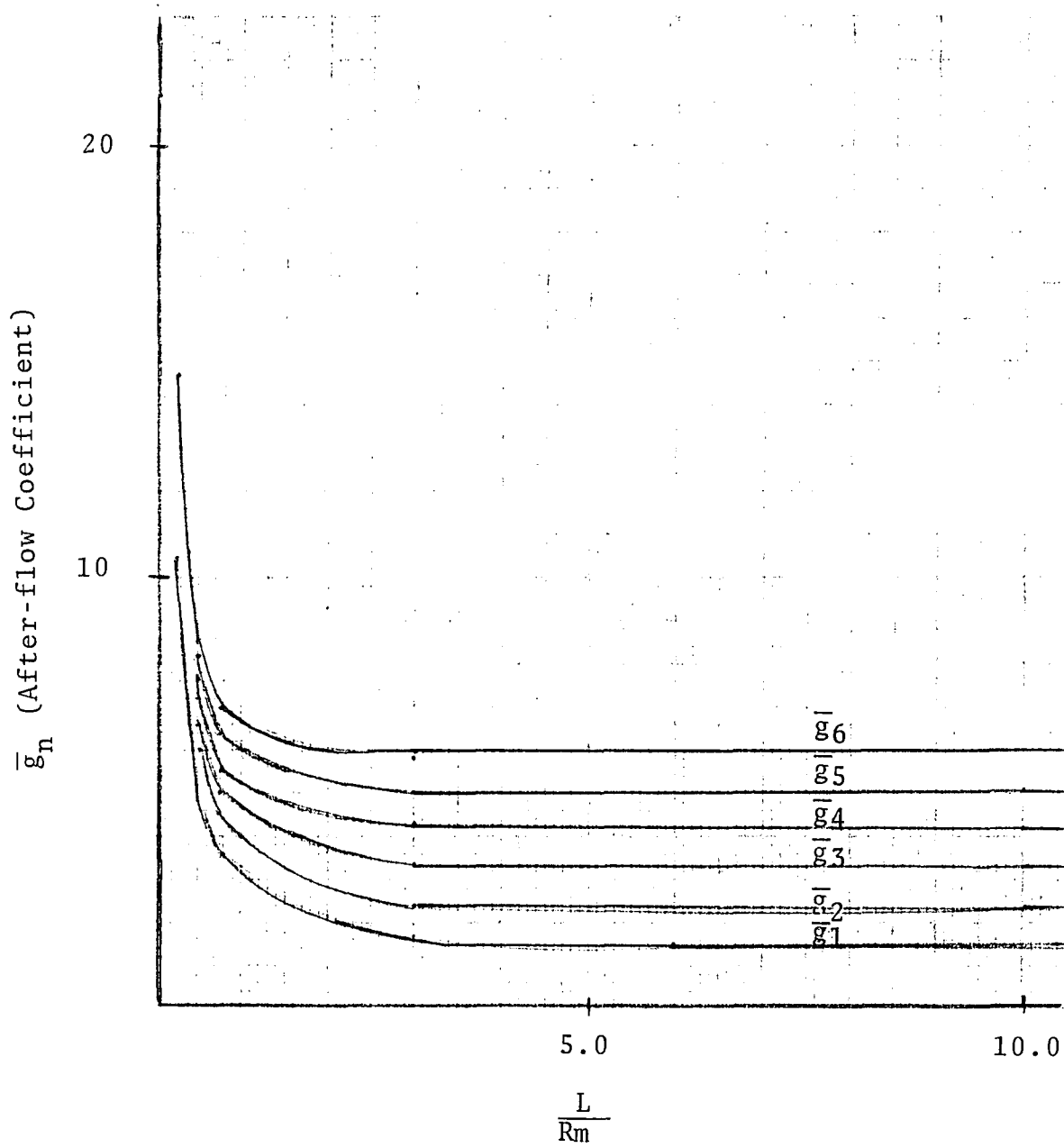


Figure 5.1 - The after-flow coefficient

## CHAPTER 6

CONCLUSIONS

The natural frequencies of a submerged, ring-stiffened, cylindrical shell of finite length considering the prestress and the effect of eccentricity were analyzed.

The dynamic interaction between the stiffened cylinder and the acoustic medium is found to have a very significant effect on the system's vibration characteristics. In contrast to McElman's analytical method, reference [3], the present study considered the boundary conditions of the fluid-structure interface as well as all three degrees of freedom of vibration. The present method gives significantly lower frequencies in water (Table I).

The fluid-structure interaction, in another point of view, may be considered as added mass. Compared to the total effective mass of the system, the portion of ring distributed mass is smaller when the system is in water and is larger when the system is in a vacuum. Therefore, the present analytical procedure is capable of yielding accurate natural frequencies in water when the ring spacing,  $\lambda$ , is sufficiently small to be averaged out.

There is a limitation to the McElman's method and any other orthotropic approach. It is that a high circumferential mode shape may not be approximated by an overall longitudinal mode shape [4]. Therefore, some of the high mode natural frequencies deviate substantially from the actual values. This limitation also applies to the present analysis, as discussed in Chapter 5.

## CHAPTER 7

RECOMMENDATION

The differential equilibrium equations are derived for a thin, circular cylindrical shell with evenly spaced uniform stiffeners submerged in a fluid medium. It is assumed that the stiffener spacing is small compared with the vibration wave length in order that its effect on the behavior of the structure may be averaged or distributed. Therefore, the deformation of the ring stiffener in this study is not considered independently. For future studies, it is recommended that the shell elements and stiffeners be considered as separate structures and that compatibility be enforced at their junctures.

REFERENCES

- [1] J. W. S. Rayleigh, The Theory of Sound, New York: Dover Publications, 1945.
- [2] A. E. H. Love, Treatise on the Mathematic Theory of Elasticity, New York: Dover Publications, 1944.
- [3] J. A. McElman, M. M. Mikulas, Jr., and M. Stein, "Static and Dynamic Effects of Eccentric Stiffening of Plates and Cylindrical Shells," AIAA Journal, vol. 4, No. 5, May, 1966, pp. 887-894.
- [4] A. Harari and M. L. Baron, "Analysis for the Dynamic Response of Stiffened Shells," Journal of Applied Mechanics, vol. 40, Trans. ASME, vol. 95, Series E, 1973, pp. 1085-1090.
- [5] M. C. Junger, "Radiation Loading of Cylindrical and Spherical Surface," Journal of the Acoustical Society of America, vol. 24, May, 1952, pp. 288.
- [6] M. C. Junger, "The Physical Interpretation of the Expression for an Outgoing Wave in Cylindrical Coordinates," Journal of the Acoustical Society of America, vol. 25, January, 1953, pp. 40.
- [7] M. C. Junger, "Vibrations of Elastic Shell in a Fluid Medium and the Associated Radiation of Sound," Journal of Applied Mechanics, Trans. ASME, vol. 74, 1952, pp. 439-445.
- [8] H. Herman and J. M. Klosner, "Transient Response of a Periodically Supported Cylindrical Shell Immersed in a Fluid Medium," Journal of Applied Mechanics, vol. 32, Trans. ASME, vol. 87 Series E, 1965, pp. 562-568.
- [9] W. C. Lyons, J. E. Russell, and G. Herrmann, "Dynamics of Submerged Reinforced Cylindrical Shell," Journal of the Engineering Mechanics Division, ASCE, vol. No. EM2, proc., April, 1968, pp. 397-420

- [10] R. B. Paslay, R. B. Tatce, R. J. Wernick, E. K. Walsh, and D. F. Muster, "Vibration Characteristics of a Submerged Ring-Stiffened Cylindrical Shell of Finite Length," The Journal of the Acoustical Society of America, vol. 46, No. 3 (part 2), 1969, pp. 701-710.
- [11] L. Prandtl and O. G. Tietjens, Fundamentals of Hydro-and-Aeromechanics, New York: Dover Publications, 1957, p. 131.
- [12] S. P. Timoshenko and J. M. Gere, Theory of Elastic Stability, New York: McGraw-Hill Book Company, 1964, pp. 265-443.
- [13] H. L. Langhaar, Energy Methods in Applied Mechanics, New York: John Wiley and Sons, Inc., 1962,
- [14] M. Abramowitz and I. A. Stegun, Handbook of Mathematical Functions Applied Mathematic Series 55, Washington, D.C.: National Bureau of Standards, 1964,
- [15] L. F. Shampine and R. C. Allen, Jr., Numerical Computing, Philadelphia: W. B. Saunders Co., 1973.
- [16] M. Pappas and A. Allentuch, Optimal Design of Submersible Frame Stiffened, Circular Cylindrical Hulls, NCE Report No. NV6 (Revised), July, 1972.
- [17] S. Hayek and D. S. Pallett, "Theoretical and Experimental Studies of the Vibration of Fluid Loaded Cylindrical Shells," Symposium on Application of Experimental and Theoretical Structural Dynamics, Southampton University, England, Apr. 1972.
- [18] H. H. Bleich, "Approximate Determination of the Frequencies of Ring-Stiffened Shells," Osterreichishes Ingenieur-Archiv, vol. XV, 1961.
- [19] G. D. Galletly, "on the In Vacuo Vibration of Simply Supported Ring-Stiffened Cylindrical Shells," Proceedings, 2nd U.S. National Congress of Applied Mechanics, p. 225ff.
- [20] T. Wah, "Flexural Vibration of Ring-Stiffened Cylindrical Shells," Journal of Sound and Vibration, vol. 3, No. 3, 1966, p. 242ff.



- [21] N. L. Basdekas and M. Chi, "Response of Oddly Stiffened Circular Cylindrical Shells," Journal of Sound and Vibration, vol. 17, pp. 187-206.
- [22] A. N. Tikhonov and A. A. Samarskii, Equation of Mathematical Physics, New York: The MacMillan Co., 1963, Chapter VII.
- [23] J. H. Haywood, "Response of an Elastic Cylindrical Shell to Pressure Pulse," The Quarterly Journal of Mechanics and Applied Mathematics, vol. II, part 2, 1958, pp. 129-141.

VITA

Author: Kerry Kier-Ten Chu

Education:

Virginia Polytechnic Institute

M.S.M.E. June, 1965

Chinese Naval College of Technology

B.S.M.E. June, 1954

Professional Experience:

1967-1977

Senior Research Engineer, Solid Mechanics Department  
Research and Advanced Product Development,  
Delaval Turbine Inc., Trenton, N.J.

1965-1967

Engineer, Ship Motion Division, John J. Mullen  
Associates, Inc., New York City.

1961-1962

Instructor of Taiwan Provincial Maritime College

1954-1961

Engineer in Chinese Naval Shipyard

Technical Membership:

Member of the American Society of Mechanical Engineers.